ELSEVIER

Brain Research 865 (2000) 1–11

BRAIN RESEARCH

www.elsevier.com/locate/bres

Research report

Physiological characterization of layer III non-pyramidal neurons in piriform (olfactory) cortex of rat

Alexander D. Protopapas*, James M. Bower

Division of Biology, MS 216-76, California Institute of Technology, Pasadena, CA 91125, USA

Accepted 25 January 2000

Abstract

We performed whole-cell recordings of layer III non-pyramidal neurons in the piriform cortex of Sprague–Dawley rats. For comparison purposes, recordings were made from deep pyramidal cells, which are also present in layer III. These two cell types could be distinguished both anatomically and physiologically. Anatomically, the layer III non-pyramidal neuron displayed smooth beady dendrites, while deep pyramidal cells showed thicker dendrites with spines. The dendrites of the layer III non-pyramidal neuron also tended to be restricted to layer III while deep pyramidal cells had long apical dendrites that spanned layers I and II. Although the resting membrane potentials of both cell types were very similar, significant differences were noted in other physiological measures. Layer III non-pyramidal neurons typically displayed higher input resistances, faster time constants, smaller spike amplitudes, shorter spike widths, and higher spike thresholds. In addition, layer III non-pyramidal neurons were able to spike at much higher rates when stimulated with the same level of threshold normalized current injection. The most dramatic differences in physiology were seen in the pattern of spiking in response to increasing levels of positive constant current pulses. Layer III non-pyramidal neurons showed qualitatively different responses at low and high levels of stimulation. At low levels, spikes occurred with long latency and the firing frequency increased throughout the duration of the current pulse. At high levels, non-pyramidal neurons started spiking with short latency, followed by a decrease in firing frequency, which in turn was followed by an increase in firing frequency. Deep pyramidal neurons differed dramatically from this pattern, displaying a qualitatively similar response at all levels of current injection. This response was characterized by short latency spikes and spike adaptation for the duration of the current pulse.

Themes: Sensory systems

Topics: Olfactory senses

Keywords: Piriform (olfactory) cortex; Layer III non-pyramidal neuron; Deep pyramidal neuron; Rat

1. Introduction

Our laboratory has had a long standing interest in elucidating the function of the mammalian olfactory system through a variety of experimental and modeling methods [4,5,23,38]. One topic of great interest to us is the role of inhibitory neurons in piriform cortex. An earlier network model of piriform cortex developed in our laboratory had suggested that feedback inhibitory neurons might control the generation and amplitude of γ oscillations (30–50 Hz) and feedforward inhibitory cells might control θ oscillations (4–12 Hz) [38]. These oscillations have been shown to correlate to sniffing and exploratory behavior in awake-behaving animals [7,39].

Dual intracellular recordings definitively showing neurons in layer III eliciting IPSPs in postsynaptic cells have not yet been done. However, immunohistochemical staining of GABA- and glutamic acid decarboxylase (GAD)-containing neurons in layer III of piriform cortex suggests the presence of inhibitory neurons in that layer [12,17]. Anatomical and physiological work has also suggested that layer III interneurons may provide feedback inhibition to pyramidal cells in the piriform cortex [12,28].

Previous experimental studies of inhibitory and putative inhibitory neurons in piriform cortex have focused on synaptic properties [14,26–29,34,36], neuromodulation [8,9,19,20,30], and anatomy [12,17]. In this study, we examine the membrane properties of non-pyramidal puta-

*Corresponding author. Tel.: +1-646-602-8115; fax: +1-626-795-2088.

E-mail address: alexp@bbb.caltech.edu (A.D. Protopapas)

0006-8993/00/$ – see front matter
PII: S0006-8993(00)02070-9

tive inhibitory cells located in layer III of piriform cortex. More specifically, we describe the active and passive properties of layer III non-pyramidal neurons and contrast them with those of deep pyramidal cells, whose somata are also located in layer III. The results indicate clear physiological differences between the two cell populations. We have characterized the layer III non-pyramidal neurons in such a way that a computer modeler can easily parameterize a simple model of this cell type using the measurements provided in this paper.

2. Materials and methods

2.1. Experimental slice procedures

2.1.1. Slice preparation

Female Sprague–Dawley rats of 4–5 weeks in age were decapitated under ether anesthesia following procedures approved by the animal care and use committee at Caltech (protocol #1156). The brains were removed and bathed in cooled medium previously bubbled with 95% O_2 and 5% CO_2 during the slicing procedure. A vibratome (WPI VSL) was used to cut five coronal 400-μm thick slices from every brain starting at 0.4 mm caudal to the anterior commissure. Slices were initially incubated for 35 min at 35°C in a jar containing medium bubbled with the gas mixture described above and then transferred to vials containing medium at room temperature. The medium used to bathe the slices was made with distilled water and consisted of (in mM): $NaHCO_3$ 26, NaCl 124, KCl 5, KH_2PO_4 1.2, $CaCI_2$ 2.4, $MgSO_4$ 1.3, and dextrose 10 [1,35]. Kynurenic acid (660 μM) was added to the medium in the vials and during slicing to prevent neuronal damage due to excitotoxicity; however, medium without kynurenic acid was used to perfuse the slices over the course of experiments. During recording, the slice was placed at the bottom of a submersion-type slice chamber, with the temperature maintained at 30–35°C. Medium passed through the chamber at a rate of approximately 2.5 ml/min.

2.1.2. Cell identification

Neurons were observed with a Zeiss Axioskop microscope during approach with electrodes. All recordings were made from layer III of piriform cortex. This layer is easily identified because it is adjacent to a dense clustering of superficial pyramidal cell bodies in layer II that is visually distinguishable in the unstained slice [11]. Although the somata of layer III non-pyramidal and deep pyramidal cells were visible under the microscope, a similarity in cell body size made it impossible to distinguish the two cell types on this basis. However, physiological response properties clearly indicated two populations of neurons, which on subsequent staining revealed distinct dendritic morphologies (see Section 3).

2.2. Recording procedures

All recordings were intracellular and were done using the whole-cell technique. Electrodes had impedances of 3.0–9.5 MΩ and were filled with the following solution (in mM): potassium gluconate 120, KCl 10, EGTA 10, Hepes 10, $MgCl_2$ 2, $CaCl_2$ 2, Na_2ATP 2, with pH 7.3 (adjusted with KOH) and osmolarity 290 mOsm [18]. Each electrode was filled with solution that was first passed though a 0.02-μm filter. Only neurons with stable resting membrane potentials of <-60 mV and spike half widths of <2 ms were used for analysis. To account for the presence of diffusion potentials [3] at the electrode tip, we used the computer program JPCalc [2] to calculate junction potentials based on the ionic concentrations of our electrode and bath solutions and the temperature at which we did our experiments. Calculated junction potentials are subtracted from all recordings of membrane potential reported in this study.

An Axoclamp 2A amplifier (Axon Instruments, Foster City, CA) was used to inject current and record membrane potential. Stimulation was controlled by software developed in our laboratory, and in some cases by pClamp (Axon Instruments). Data were digitized using either a MetraByte or Digidata 1200B A/D converter and stored directly to the hard drive of a Pentium PC.

2.2.1. Anatomical staining techniques

Neurons were labeled with a 1% neurobiotin tracer (Vector Laboratories, Burlingame, CA) solution (contained in the whole-cell electrode solution described above) during physiological recordings. A 3-Hz train of constant current pulses (0.4 nA) lasting 10–15 min was used to ionophoretically inject recorded cells with tracer.

Tissue processing began by fixing the cells in 4% paraformaldehyde (in 0.1 M phosphate buffer solution (PBS)) for at least 12 h at 4°C. Slices were then rinsed three times in 0.1 M PBS before incubation (at room temperature (RT)) for 30 min in a 0.1 M PBS solution of 10% methanol and 3% hydrogen peroxide to reduce background staining by inactivating endogenous peroxidases present in blood vessels. This was followed by five rinses in 0.1 M PBS and then incubation (RT) in a 0.75% solution of Triton X-100 (Sigma, St. Louis, MO) in 0.1 M PBS for 3 h.

Sections were rinsed 5 times in 0.1 M PBS prior to an overnight incubation at 4°C in an avidin–biotin solution (four drops of solutions A and B (Vectastain ABC kit, Vector Laboratories) in 20 ml of 0.1 M PBS). The final step in the staining procedure is reaction with diaminobenzidine (DAB). DAB (2.3 mM) was dissolved in a solution of 0.05 M PBS containing 3% H_2O_2 and 1.5% $NiCl_2$. Contact between the DAB solution and the slices varied from 3 to 5 min, after which the slices were rinsed 4 times with 0.1 M PBS with the last three rinses lasting for 5 min.

We then wet-mounted our sections to take photographs and make camera lucida drawings of stained neurons.

2.2.2. Pharmacology

When required, the effects of voltage-gated currents were minimized by bathing the slices in tetrodotoxin (TTX, Sigma, St. Louis, MO) and CsCl. TTX acts to block sodium currents, while Cs^+ acts as a non-specific potassium channel blocker. In experiments where we wished to block the effects of synaptic input, 6-cyano-7-nitroquinoxaline-2,3-dione (CNQX, RBI, Natick, MA), DL-2-amino-5-phosphovaleric acid (APV, Sigma), and picrotoxin (PCTX, RBI) were used to block AMPA/kainate, NMDA, and $GABA_A$ receptors, respectively. In all cases, recording started at least 10 min following the application of any kind of blocker. Experiments indicated that this was the minimum time needed for cell properties to stabilize. In those recordings where TTX and CsCl were used, only one recording was made per slice.

2.3. Analysis of experimental data

Current versus voltage (I–V) curves were obtained for each cell by injecting a series of at least four 1-s long current pulses into the cell. Based on these measurements, cellular input resistance was calculated by taking the slope of the linear regression fit to the linear portion of the I–V curve. Values for membrane time constant were obtained by fitting an exponential to the transient portion of the neuron's response to a constant current pulse. All curve fitting was done on an UltraSparc workstation (Sun Microsystems, Palo Alto, CA) using MATLAB (MathWorks, Natick, MA) and analysis software developed in our laboratory. Statistical analysis was done using EXCEL (Microsoft, Redmond, WA).

F–I curves were obtained by calculating the inverse of the interspike interval (in Hz) and plotting this against the time of spike occurrence and the magnitude of current injection in a three-dimensional plot [1].

3. Results

The primary objective of this investigation was to physiologically characterize layer III non-pyramidal cells in piriform cortex. However, the longer term goal of these investigations is to more clearly understand the contributions made by this and other cell types to cortical computation. For that reason, we also presented data regarding the physiological properties of deep pyramidal cells (also located in layer III) recorded over the course of the same experiments. Contrasting these two cell types in the same paper with data obtained under the same conditions may aid future investigators using in vitro or in vivo techniques to distinguish between the two cell types on the basis of their physiological responses alone. Before considering the physiological differences between these two cell types, we first describe their anatomical properties.

3.1. Anatomy of neurons

When visualized during approach with a patch electrode, the somata of layer III non-pyramidal and deep pyramidal cells appear very similar in shape and size (see Fig. 1). In fact, we were seldom able to predict which type of cell we would find based on the microscope image of the unstained neuron. Unambiguous anatomical identification therefore required the use of neurobiotin to stain recorded neurons.

The morphologies of our stained cells fit into anatomical classes of layer III neurons that had been previously characterized by a Golgi study of piriform cortex [10] (see Section 4). A total of six deep pyramidal cells and two non-pyramidal cells were stained. Representative stained neurons are shown in Fig. 1. As the figure illustrates, the vast majority of the non-pyramidal cell dendrites were found in layer III of piriform cortex, with only a single dendrite making its way up to layer II. In comparison, the deep pyramidal cell shows a tuft of basal dendrites that are segregated to layer III, but also an apical dendrite with a long almost branchless stalk that begins to branch out just before entering layer II. Significant differences are seen at a smaller scale as well. The dendrites of the non-pyramidal neuron are thin compared to those of the pyramidal cell and show well-defined varicosities, while pyramidal dendrites have spines and lack varicosities. In contrast, as expected from the light microscopic view during recording sessions, the somata of the two cell types shown in Fig. 1 are very similar with diameters of 12.0 μm for the non-pyramidal neuron and 10.4 μm for the pyramidal cell. Cell body diameters were calculated by measuring the greatest distance across the soma.

3.2. Passive properties

A list of passive properties for layer III non-pyramidal and deep pyramidal neurons is shown in Table 1. Values listed in the results section are mean±S.D. All physiological parameters were determined from a sample of 19 non-pyramidal and nine pyramidal cells.

Differences in the resting membrane potentials (RMPs) of the two cell types were found to be statistically insignificant. The mean input resistance (R_{in}) of these two cell types, however, differed significantly. Layer III non-pyramidal cells were found to have an R_{in} of 84.6±32.3 MΩ, while deep pyramidal cells had a mean input resistance of 59.6±16.9 MΩ. This difference was statistically significant ($P<0.05$, Student's t-test), although there was significant overlap in the distribution of input resistance values for the two neuron types.

We also measured the time constant (τ_0) of both types of neurons using each cell's response to a −0.1-nA constant

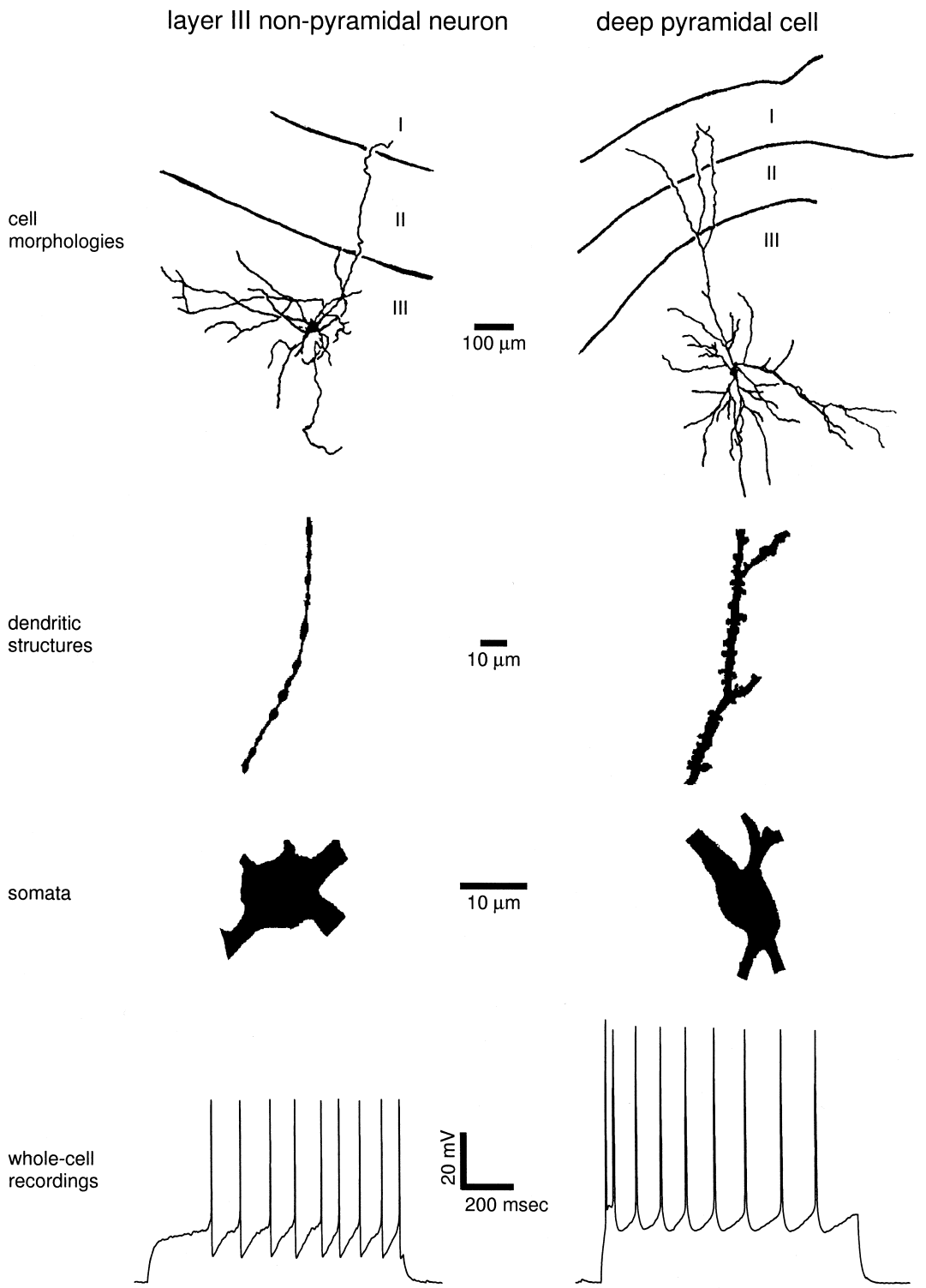

Fig. 1. The top row shows the gross morphologies of a layer III non-pyramidal cell and deep pyramidal neuron. Dendritic organization differs in that almost all non-pyramidal cell dendrites are restricted to layer III, while deep pyramidal cell dendrites are organized in a polar fashion with a tuft of basal dendrites and a thick apical stalk that bifurcates as it enters layer II. Differences in fine dendritic structure are seen in the second row. Non-pyramidal cell dendrites tend to be thinner and have multiple varicosities in contrast to the thicker spiny dendrites of the pyramidal cell; however, the somata of the two cell types have similar sizes. The bottom row shows whole-cell recordings taken from these non-pyramidal (82698a) and deep pyramidal (81898a) cells.

current injection lasting from 600 to 1000 ms. The difference in τ_0 values was large with non-pyramidal neurons having a mean value of 6.5 ± 2.3 ms and pyramidal neurons having a mean value of 12.1 ± 2.5 ms. These differences were also statistically significant ($P<0.0005$), with much less overlap in the distributions of values for

Table 1
Values are means±S.D.

	Layer III non-pyramidal cell (n=19)	Deep pyramidal cell (n=9)
RMP (mV)	−71.2±2.9	−71.4±4.3
R_{in} (MΩ)*	84.6±32.3	59.6±16.9
τ_0 (ms)***	6.5±2.3	12.1±2.5
Spike height (mV)*	73.4±12.4	87.0±9.2
Threshold (mV)*	24.1±5.7	19.3±2.0
Half-width (ms)***	0.54±0.21	1.38±0.25
Spike rate at 1×threshold (Hz)*	6.26±4.74	2.56±1.94
Spike rate at 2×threshold (Hz)***	70.5±35.5	21.6±6.3

Asterisks indicate that the difference between means is statistically significant as established by Student's t-test. Number of asterisks indicate level of statistical significance: *$P<0.05$; and ***$P<0.0005$.

the two cell types than was found, for example, in measures of input resistance.

3.3. Intrinsic and extrinsic influences on passive properties

To assess the possible role that background synaptic input might have on the passive properties of non-pyramidal neurons, we measured the passive parameters of six cells in the presence and absence of synaptic blockers (30 μM CNQX, 100 μM APV, 50 μM PCTX). Synaptic blockers changed the mean values of RMP, R_{in} and τ_0 by less than 4%. A similar lack of effect of residual synaptic activity has also been found for pyramidal cells in vitro [23]. For this reason, we did not use synaptic blockers in our passive property measurements of either cell type.

Previous studies have shown that the presence of voltage-gated channels can significantly alter the passive properties of neurons [23,25]. In order to assess the contribution of voltage-gated currents to the ostensibly passive properties of layer III non-pyramidal neurons, we measured R_{in} and τ_0 in the presence and absence of the Na^+ channel blocker TTX (1 μM) and the K^+-channel blocker Cs^+ (5 mM). Results showed R_{in} increasing on average from 80.6 MΩ (no blockers) to 104.4 MΩ (with blockers) (n=2) and τ_0 increasing from 7.2 to 12.2 ms (n=2). These results suggest that voltage-gated currents contribute significantly to the passive properties of these non-pyramidal cells. The I–V curve in Fig. 2 shows this effect in greater detail. When blockers are added to the slice, the I–V curve becomes linear over all negative current levels and up to the +0.05 nA level, suggesting that over this range TTX and Cs^+ are successful in making the neuron behave like a passive element. Over a small portion of the current range (−0.075 to 0.00 nA) the behavior of the I–V curves in the presence and absence of blockers is identical. This implies that voltage-gated currents play their largest role in subthreshold responses outside of this range. Because this property is well

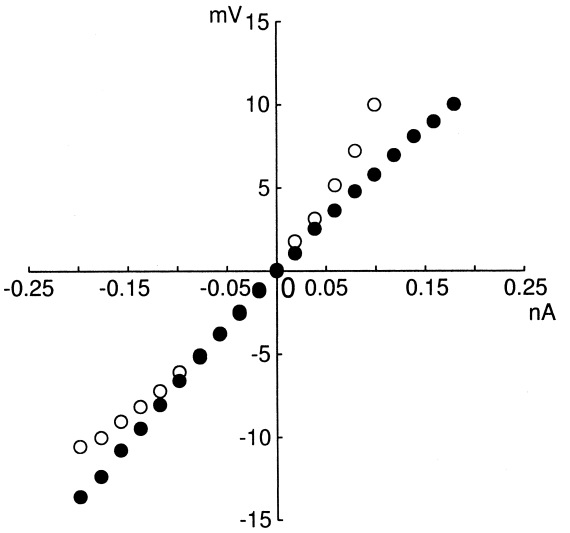

Fig. 2. I–V plot of a typical non-pyramidal neuron in the presence and absence of sodium and potassium channel blockers. Open circles show neuron's response to 600-ms constant current pulses in the absence of blockers. Filled circles indicate response of the same cell (82598c) in the presence of 5 mM CsCl and 1 μM TTX. Behavior of this neuron in the absence and presence of blockers is almost indistinguishable in the range of −0.075 to 0.0 nA, hence the overlap of points represented by open and filled circles at these levels of current injection.

described in pyramidal cells [23], we did not include this analysis in the present study.

3.4. Spike shapes

Previous studies in neocortex have described clear differences in the shapes of putative inhibitory and pyramidal cell action potentials [6,22]. Those reports showed that neocortical inhibitory neurons typically exhibited shorter spike heights and smaller spike widths. As Table 1 shows, this is also the case in piriform cortex. Differences in the mean values of spike height (non-pyramidal cell, 73.4±12.4 mV; deep pyramidal cell, 87.0±9.2 mV) and threshold (non-pyramidal cell, 24.1±5.7 ms; deep pyramidal cell, 19.3±2.0 ms) are both statistically significant ($P<0.05$), although there is overlap in the distributions of values for the two cell types. The difference in spike half-width, on the other hand, was more dramatic with non-pyramidal cells having only 39% the width of deep pyramidal cells. In this case, there was almost no overlap in individual values for the two populations.

3.5. Spiking patterns

Beyond the shape of individual spikes, the patterns of spiking generated by current injection in these two cell types is quite different. Typical responses to a 1.0-s long constant current pulse of a layer III non-pyramidal neuron and a deep pyramidal cell are shown in Fig. 3. The top set of traces shows the neurons' response to a level of current

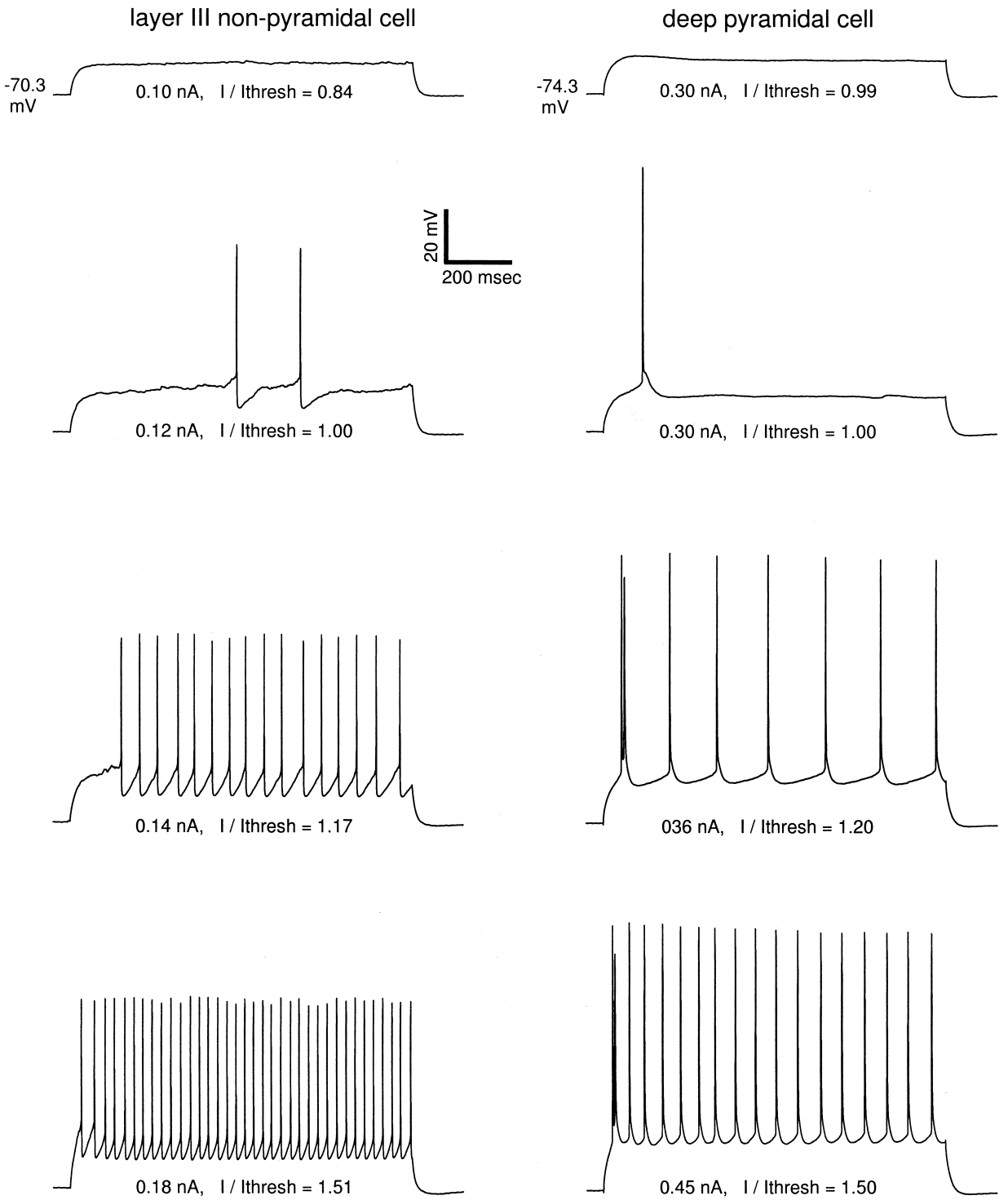

Fig. 3. Comparison of responses to current pulses in a layer III non-pyramidal neuron and a deep pyramidal cell. Top row shows the subthreshold response of a non-pyramidal neuron (82598c) and a deep pyramidal neuron (82598b). The neurons' resting membrane potential is shown to the left of each of these traces. Below each trace is the absolute level of current injection along with that level normalized to a threshold level current pulse.

injection that is just below threshold. While the layer III non-pyramidal neuron shows a very gentle ramping to more depolarized level of membrane potential, the deep pyramidal cell responds with a slight hump at the beginning of the recording followed by a slight and sustained hyperpolarization.

The second clearly noticeable difference between these neurons is in the pattern of spiking at or near threshold. In

the layer III non-pyramidal cell, two spikes are generated with long latency, while the deep pyramidal cell produces a single spike with a much shorter latency. Interestingly, the positioning of the spikes in both cases matches the relative levels of depolarization in the subthreshold response of the two cells. In the case of the layer III non-pyramidal cell, the spikes occur later in the response where the cell had become more depolarized at the subthreshold level. Similarly, the spike elicited by the deep pyramidal cell occurs just over the slight hump seen in its subthreshold response.

As greater levels of current injection are applied to these neurons, additional differences are seen. For example, at a level of current injection that is roughly 1.2 times that of the minimum suprathreshold level, the deep pyramidal cell now shows two spikes with a very small interspike interval followed by six more spikes with much longer but almost constant interspike intervals. In contrast, the non-pyramidal cell continues to show a longer latency before spiking and the interval between all 16 spikes is roughly the same and unchanging. At a level of current injection that is 1.5 times that required to elicit spiking, latency for the non-pyramidal neuron has become very short, but unlike the deep pyramidal cell, the first two spikes have the longest interspike interval in the spike train.

Fig. 4 shows the relationship between the level of current injection and the number of spikes elicited in typical layer III non-pyramidal and deep pyramidal cells. Qualitatively, both cell types show an almost linear relationship between spike count and the magnitude of a 1.0-s long constant current pulse, although the response of the deep pyramidal cell begins to saturate slightly at high levels of current injection. In these particular neurons, a greater level of absolute current was needed to cause the non-pyramidal neuron to spike as compared to the pyramidal cell; however, this was not always the case. For example, in the comparison between the two neurons in Fig. 3 the non-pyramidal neuron required less current to fire.

The most obvious difference between the neurons shown in Fig. 4 is that the non-pyramidal neuron generates far more spikes for a given level of current injection than does the pyramidal cell. This is the case even when the magnitude of current injection is normalized by the threshold current injection. Although the two neurons both respond with two spikes at a threshold level of current injection, at 3.1 times threshold the non-pyramidal neuron produces 104 spikes over the duration of a 1.0-s pulse while the deep pyramidal cell produces only 31.

To quantify changes in spiking pattern that occur over progressively higher levels of current injection, we plotted the instantaneous spiking frequency (the inverse of the interspike interval) against threshold normalized current injection and the time of occurrence of the spikes [1]. The frequency versus current (F–I) plots for two typical neurons are shown in Fig. 5. The F–I plot for the layer III

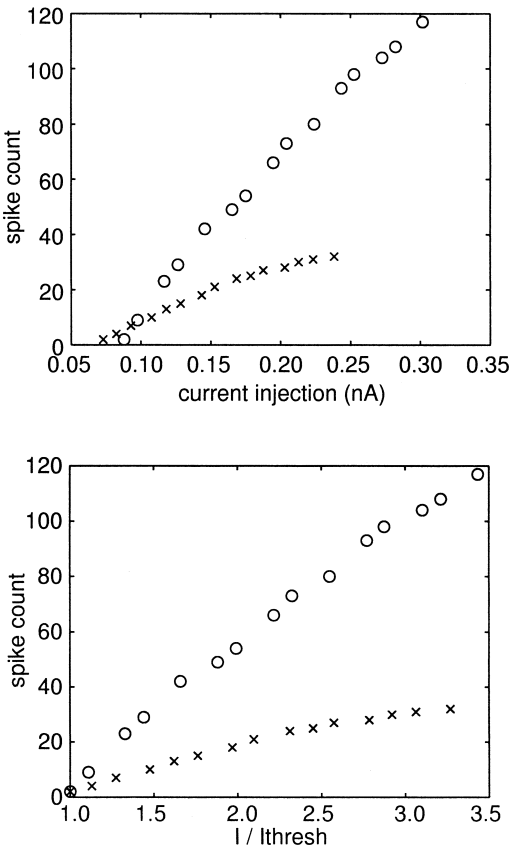

Fig. 4. Spike count versus level of current injection for a typical layer III non-pyramidal neuron and a deep pyramidal cell. Open circles represent the response of a non-pyramidal cell (72898c) and ×'s the response of a deep pyramidal cell (72298a). Points in the top figure are plotted against the absolute level of current injection, while those on the bottom are plotted against normalized current injection.

non-pyramidal neuron shows two distinct patterns of behavior that are dependent on the level of current injection. At low levels of current, the spiking pattern shows a small monotonic increase in firing frequency (i.e., a decrease in interspike interval) over the duration of the current pulse; however, at higher levels of current injection (roughly 1.4 times threshold current and greater), the spiking pattern shows an initially high frequency followed by a large drop and then a monotonic increase in frequency for the remainder of the current pulse. A set of traces comparing non-pyramidal cell spike train behavior at low and high levels of current injection is shown in Fig. 6.

In contrast, the deep pyramidal cell in Fig. 5 shows a consistent pattern of firing throughout the range of current injection. Instantaneous frequency starts very high and then drops quickly, after which a much smaller decline in frequency occurs for the remainder of the stimulus.

3.6. Influences on spiking patterns

The spiking pattern of layer III non-pyramidal neurons

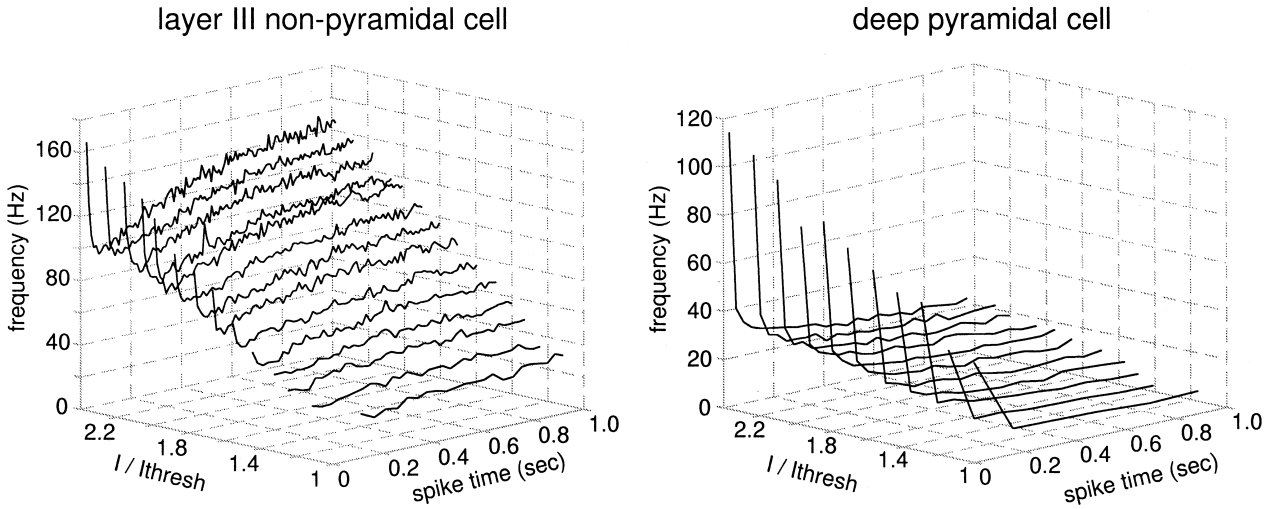

Fig. 5. *F–I* plots for a non-pyramidal (71598d) and deep pyramidal cell (72098a). The axis labeled 'spike time' indicates the time at which a spike occurs during the course of a constant current pulse while the *z*-axis shows the instantaneous frequency (inverse of interspike interval). Non-pyramidal neurons at low levels of current injection show responses that indicate a decreasing interspike interval over the course of a 1-s long constant current pulse. At higher levels of current injection, the non-pyramidal cell shows two spikes that occur with early onset and a short interspike interval. This is followed by spikes that occur with much longer spike intervals and with the progression of time the interspike interval diminishes again. In contrast, the deep pyramidal cell shows a monotonic trend in interspike interval with a very small interval separating the first two spikes followed by much longer intervals that increase more slowly. Unlike the pyramidal cell, this trend appears to be present at all levels of current injection.

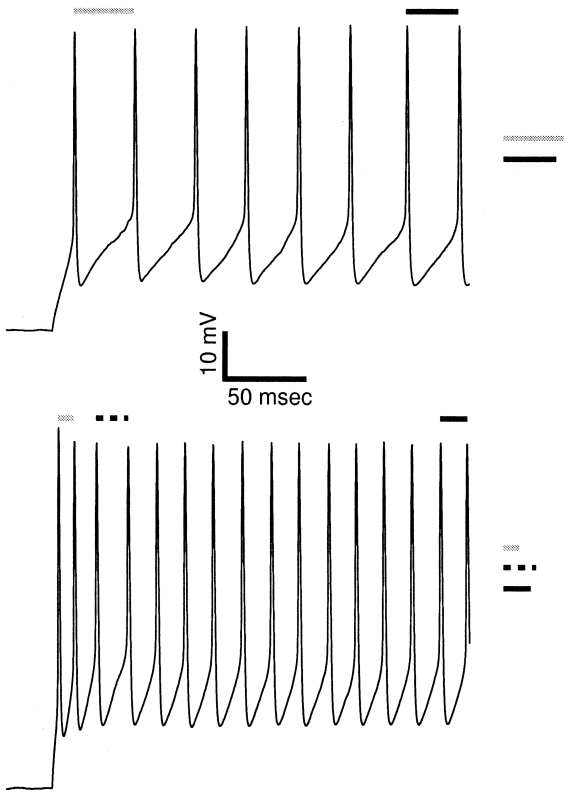

Fig. 6. Comparison of non-pyramidal cell (82698a) spike train behavior at low and high levels of current injection. At low levels of current injection interspike intervals gradually decrease as shown in the top trace. This spike train was elicited with a 0.14-nA current injection. Lower trace shows qualitatively different behavior for the same cell at greater current injection (0.25 nA). Interspike intervals increase then decrease later in the spike train.

at high levels of current injection prompted us to ask whether the decrease in frequency following the first spikes was due to intrinsic voltage-gated currents or synaptic input. Previous studies have shown that autapses are common in some inhibitory neurons [32,33]. Such self-innervation could conceivably explain the decrease in spiking frequency following the first two spikes at high levels of current injection. To test this possibility, we generated *F–I* plots in the presence and absence of synaptic blockers (30 μM CNQX, 100 μM APV, 50 μM PCTX). Blockers for the $GABA_B$ receptor were not used because the relatively long time course for this type of inhibition [16,36] makes it unlikely to account for the short latency drop in firing frequency. We found that in all cases ($n=5/5$), synaptic blockers did not qualitatively change the spiking pattern of layer III non-pyramidal neurons (see Fig. 7 for an example). However, we did find that neurons in the presence of these blockers tended to require greater levels of current to fire at rates comparable to what was seen in the absence of blockers. A similar phenomenon was observed with prolonged recordings (over 20 min) whether blockers were present or not. We suspect that this change may therefore result from electrode washout during these longer experiments (a common problem with patch electrodes [13,24]), rather than the effects of the synaptic blockers themselves.

4. Discussion

In this paper, we have characterized the response of layer III non-pyramidal neurons by measuring their passive

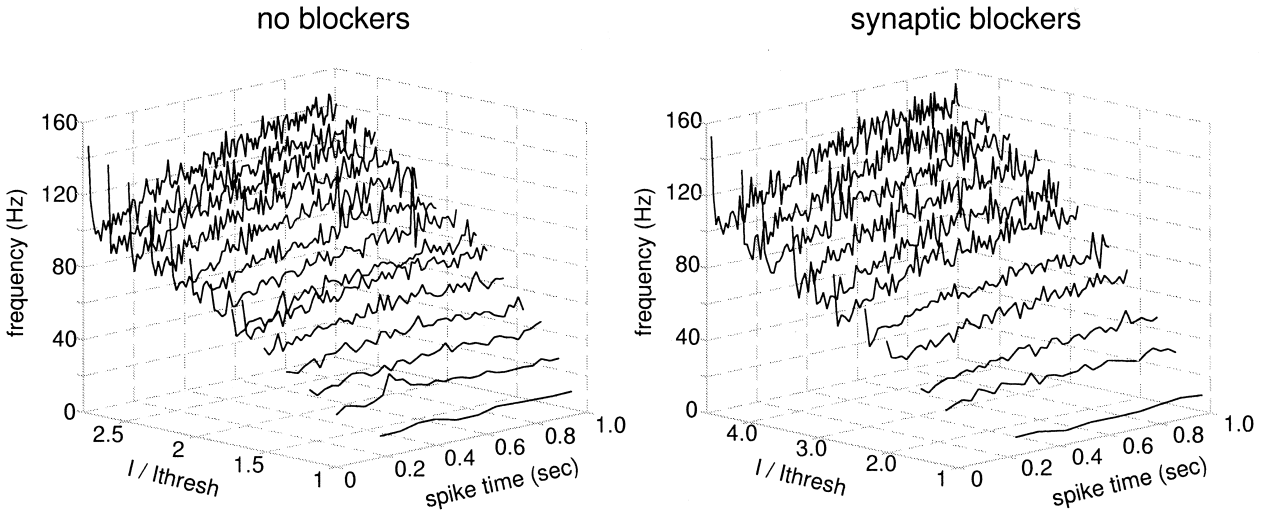

Fig. 7. *F–I* plots for a layer III non-pyramidal neuron (62498b) in the presence and absence of synaptic blockers (30 μM CNQX, 100 μM APV, 50 μM PCTX). These experiments were done to test the possibility that the initial decrease in instantaneous frequency at high levels of current injection is the result of synaptic input. The presence of synaptic blockers does not appear to have an effect on qualitative features of the spiking pattern; however, it seems that the neuron is less excitable in the presence of synaptic blockers. This is most likely an artifact due to washout that has occurred over the time period separating the recordings before and after the application of blockers.

and active responses to current injection using whole-cell recording. To distinguish their physiological properties from other neurons in layer III, we also recorded from deep pyramidal cells. While non-pyramidal and deep pyramidal cells displayed similar RMPs, statistically significant differences were found for values of spike height, spike half-width, threshold, input resistance, and time constant. In addition, we compared the dynamic responses of each cell type to a range of current injections. Layer III inhibitory cells were able to fire at much higher frequencies than deep pyramidal cells stimulated at the same level of threshold normalized current injection. Spike patterns elicited at different levels of current injection also differed for the two cell types. Inhibitory neurons showed a monotonic increase in instantaneous firing frequency over the duration of a constant current pulse; however, at higher levels of current injection, these cells exhibited an initially high instantaneous firing frequency followed by a fall and then a steady increase for the duration of the current pulse. In contrast, deep pyramidal cells showed a qualitatively similar response over all levels of current injection, with a high instantaneous frequency followed by a large initial decrease and then a slower decrease in frequency for the remainder of the current injection.

4.1. Comparison to previous deep pyramidal cell studies

Deep pyramidal neurons can be distinguished from superficial pyramidal cells on both physiological and morphological grounds [35,37]. Deep pyramidal cells have long, almost branchless apical stalks and somata that are located in layer III [10,37]. In contrast, superficial pyramidal cells have somata in layer II and apical stalks that branch almost immediately after leaving the soma [10,37]. In terms of physiology, the deep pyramidal cell shows greater spike adaptation and a lower spike threshold than superficial pyramidal neurons [35].

Tseng and Haberly previously characterized the membrane properties of deep pyramidal cells using sharp electrode techniques and a slice bath solution identical to ours [35]. In general, these results were similar to those reported here, despite our use of the whole-cell technique. For example, our measurements of RMP, spike amplitude, spike duration, and threshold differed from those of Tseng and Haberly by less than 10%. However, we recorded values for input resistance and membrane time constant that were 25 and 23% greater, respectively. This divergence is likely due to the smaller electrical leak experienced by the cell when recording with whole-cell electrodes [31].

4.2. Comparison of non-pyramidal neurons to known inhibitory neurons

Neocortical studies in the 1980s and early 1990s suggested that inhibitory and excitatory neurons could be differentiated on the basis of morphology and physiological response to constant current pulses [6,15,22]. For example, neurons with pyramidal or spiny stellate morphologies were found to exhibit spike adaptation and were presumed to be excitatory. These neurons were classified as ‘regular spiking’. In contrast, neurons with aspiny or sparsely spiny non-pyramidal anatomy and fast, non-adapting spike trains were presumed to be inhibitory. These neurons were referred to as ‘fast spiking’. A more recent dual intracellular recording study by Thomson et al. [33]

has shown that some regular spiking neurons are capable of eliciting IPSPs in pyramidal cells, thus suggesting that a neuron's firing pattern is not sufficient to determine its status as an excitatory or inhibitory cell. Despite this, we know of no studies that have shown fast spiking neurons to elicit EPSPs in postsynaptic neurons.

The characteristics of layer III non-pyramidal cells in piriform cortex are similar to those of presumed inhibitory cells in hippocampus [15] and neocortex [22]. Like presumed inhibitory cells in these areas, layer III non-pyramidal cells have beady aspiny dendrites, low amplitude short-duration spikes, and lack the spike train adaptation commonly seen in cortical pyramidal cells. One aspect of layer III non-pyramidal cell behavior that we were not able to find in other cortical studies was the decrease and then increase in spike frequency that we saw at high levels of current injection. However, it is possible that such behavior is present in some hippocampal and neocortical interneurons, but that the proper level of current injection has not been used to elicit this effect in past studies.

4.3. Comparison to inhibitory cell studies in piriform cortex

Previous reports have suggested the existence of inhibitory neurons in layer III of piriform cortex. An anatomical study had shown neurons that displayed immunoreactivity to GABA in layer III [12]. Extracellular in vivo and in vitro experiments revealing populations of fast spiking neurons with low-amplitude short-duration spikes also suggested the presence of inhibitory neurons in layer III [19–21].

The layer III non-pyramidal neuron described here is aspiny with beady dendrites. An anatomical study of piriform cortex using the Golgi stain revealed neurons in layer III that had similar anatomical characteristics [10]. Although this study did not determine the inhibitory nature of these neurons, this type of morphology is similar to GABAergic neurons in other cortical areas [22,33]. One suggestion that our non-pyramidal neuron may be inhibitory comes from a study of GABA- and GAD-immunoreactivity in piriform cortex, which showed staining of large somata in layer III [12]. Non-pyramidal cells were similarly found to have large somata as observed during electrode placement under microscopic visual guidance.

Although some previous studies suggest the existence of piriform cortex inhibitory neurons in the border region of layers II and III in rat [9,30], sharp electrode recordings from these cells show spike shapes and patterns of firing that reveal that this population of neurons may be distinct from the layer III non-pyramidal cells that we have characterized here. For example, intracellular traces from layer II/III interneurons show greater spike heights and larger post-spike hyperpolarizations than those reported here for layer III non-pyramidal cells [30]. However, a study of presumed inhibitory neurons in layer III of the piriform cortex of rabbit shows intracellular traces displaying spike shapes that are qualitatively similar to those seen in our layer III non-pyramidal cells [28]. Action potentials in that study were elicited with EPSPs, making a comparison to the subthreshold and spike train behavior of our non-pyramidal cells (stimulated using constant current pulses) more difficult.

Acknowledgements

This work was supported by the Office of Naval Research as part of the Multidisciplinary Research Program of the University Research Initiative (MURI grant # DAAG55-98-0266). We wish to thank M.C. Vanier for his useful comments on the manuscript.

References

[1] B. Barkai, M.E. Hasselmo, Modulation of the input/output function of rat piriform cortex pyramidal cells, J. Neurophysiol. 72 (2) (1994) 644–658.
[2] P.H. Barry, JPCalc, a software package for calculating liquid junction potential corrections in patch-clamp, intracellular, epithelial and bilayer measurements and for correcting junction potential measurements, J. Neurosci. Methods 51 (1994) 107–116.
[3] P.H. Barry, J.W. Lynch, Liquid junction potentials and small cell effects in patch-clamp analysis, J. Membrane Biol. 121 (1991) 101–117.
[4] U.S. Bhalla, J.M. Bower, Exploring parameter space in detailed single neuron models: simulations of the mitral and granule cells of the olfactory bulb, J. Neurophysiol. 69 (6) (1993) 1948–1965.
[5] U.S. Bhalla, J.M. Bower, Multiday recordings from olfactory bulb neurons in awake freely moving rats: spatially and temporally organized variability in odorant response properties, J. Comput. Neurosci. 4 (3) (1997) 221–256.
[6] B.W. Connors, M.J. Gutnick, Intrinsic firing patterns of diverse neocortical neurons, Trends Neurosci. 13 (1990) 99–104.
[7] W.J. Freeman, Correlation of electrical activity of prepyriform cortex and behavior in cat, J. Neurophysiol. 23 (1960) 111–131.
[8] R.L. Gellman, G.K. Aghajanian, Pyramidal cells in piriform cortex receive a convergence of inputs from monoamine activated GABAergic interneurons, Brain Res. 600 (1) (1993) 63–73.
[9] R.L. Gellman, G.K. Aghajanian, Serotonin receptor-mediated excitation of interneurons in piriform cortex: antagonism by atypical antipsychotic drugs, Neuroscience 58 (1994) 515–525.
[10] L.B. Haberly, Structure of the piriform cortex of the opossum. I. Description of neuron types with Golgi methods, J. Comp. Neurol. 213 (1983) 163–187.
[11] L.B. Haberly, Olfactory cortex, in: G.M. Shepherd (Ed.), The Synaptic Organization of the Brain, 4th Edition, Oxford University Press, New York, 1998, pp. 377–416, Ch. 10.
[12] L.B. Haberly, D.J. Hansen, S.L. Feig, S. Presto, Distribution and ultrastructure of neurons in opossum piriform cortex displaying immunoreactivity to GABA and GAD and high-affinity tritiated GABA uptake, J. Comp. Neurol. 266 (1987) 269–290.
[13] R. Horn, A. Marty, Muscarinic activation of ionic currents measured by a new whole-cell recording method, J. Gen. Physiol. 92 (1988) 145–159.
[14] E.D. Kanter, A. Kapur, L.B. Haberly, A dendritic $GABA_A$-mediated

IPSP regulates facilitation of NMDA-mediated responses to burst stimulation of afferent fibers in piriform cortex, J. Neurosci. 16 (1) (1996) 307–312.
[15] Y. Kawaguchi, K. Hama, Physiological heterogeneity of nonpyramidal cells in rat hippocampal CA1 region, Exp. Brain Res. 72 (1988) 494–502.
[16] D.S.F. Ling, L.S. Benardo, Properties of isolated $GABAB_B$-mediated inhibitory postsynaptic currents in hippocampal pyramidal cells, Neuroscience 63 (4) (1994) 937–944.
[17] W. Loscher, H. Lehmann, U. Ebert, Differences in the distribution of GABA- and GAD-immunoreactive neurons in the anterior and posterior piriform cortex of rats, Brain Res. 800 (1998) 21–31.
[18] C. Major, A.U. Larkman, P. Jonas, B. Sakmann, J.J.B. Jack, Detailed passive cable models of whole-cell recorded CA3 pyramidal neurons in rat hippocampal slices, J. Neurosci. 14 (8) (1994) 4613–4638.
[19] G.J. Marek, G.K. Aghajanian, α_{1B}-Adrenoceptor-mediated excitation of piriform cortical interneurons, Eur. J. Pharmacol. 305 (1996) 95–100.
[20] G.J. Marek, G.K. Aghajanian, LSD and the phenethylamine hallucinogen DOI are potent partial agonists at $5\text{-}HT_2A$ receptors on interneurons in rat piriform cortex, J. Pharmacol. Exp. Ther. 278 (1996) 1373–1382.
[21] J. McCollum, J. Larson, T. Otto, F. Schottler, R. Granger, G. Lynch, Short-latency single unit processing in olfactory cortex, J. Cogn. Neurosci. 3 (3) (1991) 293–299.
[22] D.A. McCormick, B.W. Connors, J.W. Lighthall, D.A. Prince, Comparative electrophysiology of pyramidal and sparsely spiny stellate neurons of the neocortex, J. Neurophysiol. 54 (4) (1985) 782–806.
[23] A.D. Protopapas, J.M. Bower, The responses of layer II pyramidal cells in piriform (olfactory) cortex to current injection: a combined in vitro and computer modeling study, 2000 (submitted).
[24] M. Pusch, B. Neher, Rates of diffusional exchange between small cells and a measuring patch pipette, Pflügers Arch. 411 (1988) 204–211.
[25] M. Rapp, I. Segey, Y. Yarom, Physiology, morphology, and detailed passive models of guinea-pig cerebellar Purkinje cells, J. Physiol. 474 (1994) 101–118.
[26] M. Satou, K. Mori, Y. Tazawa, S.F. Takagi, Long lasting disinhibition in pyriform cortex of the rabbit, J. Neurophysiol. 48 (1982) 1157–1163.
[27] M. Satou, K. Mori, Y. Tazawa, S.F. Takagi, Two types of postsynaptic inhibition in pyriform cortex of the rabbit: fast and slow inhibitory postsynaptic potentials, J. Neurophysiol. 48 (1982) 1142–1156.
[28] M. Satou, K. Mori, Y. Tazawa, S.F. Takagi, Interneurons mediating fast postsynaptic inhibition in pyriform cortex of the rabbit, J. Neurophysiol. 50 (1983) 89–101.
[29] M. Satou, K. Mori, Y. Tazawa, S.F. Takagi, Neuronal pathways for activation of inhibitory interneurons in pyriform cortex of the rabbit, J. Neurophysiol. 50 (1983) 74–88.
[30] P.W. Sheldon, G.K. Aghajanian, Excitatory responses to serotonin (5-HT) in neurons of the rat piriform cortex: evidence for mediation by $5\text{-}HT_{1C}$ receptors in pyramidal cells and $5\text{-}HT_2$ receptors in interneurons, Synapse 9 (1991) 208–218.
[31] K.J. Staley, T.S. Otis, I. Mody, Membrane-properties of dentate gyrus granule cells: a comparison of sharp microelectrode and whole-cell recordings, J. Neurophysiol. 67 (5) (1992) 1346–1358.
[32] G. Tamás, E.H. Buhl, P. Somogyi, Massive autaptic self-innervation of GABAergic neurons in cat visual cortex, J. Neurosci. 17 (1997) 6352–6364.
[33] A.M. Thomson, D.C. West, J. Hahn, J. Deuchars, Single axon IPSPs elicited in pyramidal cells by three classes of interneurones in slices of rat neocortex, J. Physiol. 496 (1996) 81–102.
[34] G. Tseng, L.B. Haberly, A synaptically mediated K^+ potential in olfactory cortex: characterization and evidence for interneuronal origin, Soc. Neurosci. Abstr. 12 (1986) 667.
[35] G. Tseng, L.B. Haberly, Deep neurons in piriform cortex. II. Membrane properties that underlie unusual synaptic responses, J. Neurophysiol. 62 (1989) 386–400.
[36] G.F. Tseng, L.B. Haberly, Characterization of synaptically mediated fast and slow inhibitory processes in piriform cortex in an in vitro slice preparation, J. Neurophysiol. 59 (5) (1988) 1352–1376.
[37] G.F. Tseng, L.B. Haberly, Deep neurons in piriform cortex. I. Morphology and synaptically evoked-responses including a unique high-amplitude paired shock facilitation, J. Neurophysiol. 62 (2) (1989) 369–385.
[38] M. Wilson, J.M. Bower, Cortical oscillations and temporal interactions in a computer simulation of piriform cortex, J. Neurophysiol. 67 (1992) 981–995.
[39] D.E. Woolley, P.S. Timiras, Prepyriform electrical activity in the rat during high altitude exposure, Electroencephalogr. Clin. Neurophysiol. 18 (1965) 680–690.